Food Chemistry: X 21 (2024) 101075

Contents lists available at ScienceDirect

Food Chemistry: X

journal homepage: www.sciencedirect.com/journal/food-chemistry-x

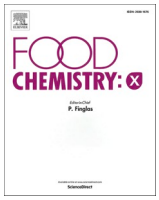

Grafting chlorogenic acid enhanced the antioxidant activity of curdlan oligosaccharides and modulated gut microbiota

Huan Li [a], Wenjiang He [b], Saiqing Xu [a,c], Rongrong Wang [d], Shuai Ge [a,c], Haishan Xu [a,c], Yang Shan [a,c], Shenghua Ding [a,c,*]

[a] DongTing Laboratory, Hunan Agricultural Product Processing Institute, Hunan Academy of Agricultural Sciences, Hunan Provincial Key Laboratory for Fruits and Vegetables Storage Processing and Quality Safety, Changsha, 410125, China
[b] R&D Centre, Infinitus (China) Company Ltd., Guangzhou, 510520, China
[c] Longping Branch, College of Biology, Hunan University, Changsha, 410125, China
[d] College of Food Science and Technology, Hunan Agricultural University, Changsha, 410128, China

ARTICLE INFO

Keywords:
Chlorogenic acid
Curdlan oligosaccharides
Antioxidant activity
Gut microbiota

ABSTRACT

In this study, the effects of grafting chlorogenic acid (CA) on the antioxidant and probiotic activities of curdlan oligosaccharides (CDOS) were investigated. CDOS with degrees of polymerization of 3–6 was first obtained by degradation of curdlan with hydrogen peroxide and then grafted with CA using a free radical-mediated method under an ultrasonication-assisted Fenton system. The thermal stability and antioxidant ability of CDOS were enhanced after grafting with CA. *In vitro* fermentation, supplementation of CDOS-CA stimulated the proliferation of *Prevotella* and *Faecalibacterium* while inhibiting the growth of harmful microbiota. Notably, the concentration of total short-chain fatty acids and the relative abundance of beneficial bacteria markedly increased after fermentation of CDOS-CA, indicating that CA grafting could improve the probiotic activity of CDOS. Overall, the covalent binding of CDOS and CA could enhance the antioxidant and probiotic activities of CDOS, suggesting potential improvements in gastrointestinal and colonic health.

1. Introduction

The dysbiosis of gut microbiota and oxidative stress are commonly associated with various human intestinal diseases, including inflammatory bowel disease and colorectal cancer (Liu, Zou, Xie, Meng, & Xu, 2023). Increasingly, evidence has indicated that polyphenols and polysaccharides may improve intestinal health by modulating the gut microbiota. Polyphenols possess excellent free radical scavenging ability (Li et al., 2021), which can be used as efficient antioxidants to mitigate oxidative damage by removing free radicals (Zhang et al., 2023). Specifically, chlorogenic acid (CA) is a functional phenolic acid abundant in potatoes, apples, honeysuckle, coffee beans, and other plants (Li et al., 2022a). CA is one of the major polyphenols in the human diet that exhibited many positive biological activities (Limwachiranon et al., 2020), including the alleviation of oxidative stress, reduction of free radical damage, mitigation of intestinal inflammation, and promotion of gut homeostatic balance (Wan et al., 2021). As a result, CA is widely utilized in food and medicine-related fields. However, CA was limited by its low stability, susceptibility to oxidation, and chemical degradation during gastrointestinal digestion, leading to a poor oral bioavailability (Zhou et al., 2022).

The polysaccharide-polyphenols interactions can stabilize the antioxidant activities, protect polyphenols from degradation, and enhance the targeted delivery of polyphenols in the gastrointestinal tract, thereby improving the gastrointestinal stability, bioavailability, biological activity, and bioaccessibility of polyphenols (Li et al., 2022b; Limwachiranon et al., 2020). Recently, there are increasing attention to the synthesis of oligosaccharides-polyphenols conjugates by grafting polyphenols onto oligosaccharide chains (Li et al., 2022b; Xiao et al., 2022). The oligosaccharides-polyphenols conjugates showed excellent gut fermentability in the colon, where they were degraded by the gut microbiota into oligosaccharides and free small phenolic acids with enhanced biological activity (Li et al., 2022b). Curdlan (CD), a linear β-glucan with β-(1 → 3) glycosidic bonds, is an indigestible bacterial polysaccharide approved as food additive by the Food and Drug Administration (Verma et al., 2020). It has been reported that curdlan supplementation could increase intestinal short-chain fatty acid (SCFA) levels, affect the intestinal microbial composition, improve the immune system, and thereby

* Corresponding author.
E-mail address: shhding@hotmail.com (S. Ding).

https://doi.org/10.1016/j.fochx.2023.101075
Received 13 July 2023; Received in revised form 10 December 2023; Accepted 13 December 2023
Available online 16 December 2023

benefiting the host by the regulation of the intestinal environment (Watanabe, Yamano, Masujima, Ohue-Kitano, & Kimura, 2021). However, curdlan is water-insoluble owing to its rigid triple helix structure, significantly limiting its application in the food and biomedical fields (Yan et al., 2020). Various methods, such as enzymic or acidic treatment (Grandpierre, Janssen, Laroche, Michaud, & Warrand, 2008), ultrasonic degradation (Li et al., 2022c), and hydrogen peroxide (H_2O_2) degradation (Zhu & Wu, 2019) had been used to produce water-soluble curdlan oligosaccharides (CDOS). Especially, H_2O_2 degradation of curdlan receives growing interest due to its low cost, high degradation efficiency, and environmental friendliness (Li et al., 2019). CDOS degraded from curdlan exhibited higher water solubility, prebiotic activity, immunostimulatory, and other biological activities compared to curdlan itself (Yan et al., 2020). Moreover, CDOS exhibited tolerance against digestive enzymes and pH in the gastrointestinal tract as well as can promote the proliferation of *Lactobacillus* sp. and *Bifidobacterium* sp. (Shi et al., 2018). Currently, little is known about the effect of CA grafting on the biological activity of CDOS. Therefore, it is hypothesized that the binding of CA to CDOS could protect CA against oxidation, as well as enhance the antioxidant and prebiotic activities of CDOS.

In the present study, considering Fenton-system medicated method possesses many advantages, such as being simple, economically friendly, and sustainable, a free radical-induced grafting approach under ultrasonication-assisted Fenton-system was used to conjugate CA with CDOS (Xu et al., 2023). The synthesized compound was characterized using UV–vis, Fourier transform infrared (FTIR), differential scanning calorimetry (DSC), and thermal gravimetric analysis (TGA). Additionally, the antioxidant activity of CDOS-CA during *in vitro* digestive process was investigated. Furthermore, the prebiotic effects of CDOS-CA were also investigated by *in vitro* human fecal fermentation. These investigations aim to provide valuable insights into the impacts of grafting CA on the biological activity of CDOS, the bioaccessibility of CDOS-CA, and the potential benefits of CDOS-CA for gut health.

2. Materials and methods

2.1. Materials

Curdlan (91 %, molecular weight = 1312.69 kDa) was purchased from Weiling Food Technology Co., LTD (Wuxi, China). CA (98 %) was the product of Shanghai Yuanye Biotechnology Co. LTD. 1, 1-diphenyl-2-picryl-hydrazyl (DPPH) was provided by Sigma-Aldrich (Germany). 2, 2′-azino-bis (3-ethylbenzothiazoline-6-sulfonic acid) (ABTS) and 2, 4, 6-tris (2-pyridyl)-s-triazine (TPTZ) were acquired from Aladdin reagent Co., LTD (Shanghai, China). Folin-Ciocalteu reagent and other reagents were bought from Sinopharm Reagent Chemical Co. LTD (Jiangsu, China).

2.2. Oxidative degradation of curdlan

CDOS was prepared by the H_2O_2 hydrolysis of curdlan according to a previously described method with modifications (Zhu et al., 2019). Curdlan (10 g) was dissolved in 2.5 M NaOH solutions (200 mL), and this solution was slowly added with 2 % (v/v) H_2O_2. Mixtures were magnetically stirred at 60 °C for 15 min. The hydrolysates were cooled and neutralized with 6 M HCl. After centrifugation at 12,000 × *g* for 15 min, the CDOS in the supernatants was placed in a 1000 Da dialysis bag and then dialyzed against ultrapure water for 72 h. Finally, CDOS was obtained by freeze-drying for further analysis. The molecular weight (Mw) of native CD was determined by a multi-angle laser light scattering gel chromatography system (SEC-MALLS, Wyatt Technology, USA). The MALDI-TOF mass spectrometry of CDOS was performed on an ultrafleXtreme instrument to analyze the Mw of CDOS (Bruker, USA) (Li et al., 2019).

2.3. Synthesis of CDOS-CA conjugate

The synthesis of CDOS-CA conjugates was prepared based on the Vc/H_2O_2 free radical-mediated method under ultrasonication-assisted Fenton-system as described by Xu et al. with minor modifications (Xu et al., 2023). In brief, 2 g CDOS was dissolved in 200 mL ultrapure water, after which 0.8 g Vc and 4 g CA (dissolved in ethanol solution) were successively added, and magnetically stirred in a nitrogen atmosphere for 30 min (Cai et al., 2019). Then, 16 mL of 5 M H_2O_2 solution was added dropwise into the mixture to trigger an oxidation reaction. Ultrasound treatment was immediately carried out in an ultrasonic bath (Kun Shan Ultrasonic Instruments Co., Ltd, Jiangsu, China) at 20 °C for 2 min under an uninterrupted nitrogen atmosphere to facilitate the reaction (Xu et al., 2023). After the reaction, the resulting mixture was centrifuged at 8000 × *g*, 4 °C for 20 min to remove the unreacted free CA. The supernatants were transferred to a dialysis bag (MWCO: 500 Da) dialyzed against 50 % ethanol for 24 h, and then dialyzed against ultrapure water for 3 d.

2.4. Characterization of CDOS-CA conjugates

2.4.1. Determination of the grafting ratio of CDOS-CA

The grafting rate of CDOS-CA conjugates was evaluated by the Folin-Ciocalteu method (Xiao et al., 2022). Briefly, 0.5 mL CDOS-CA conjugate solution (1 mg/mL) was mixed with 1 mL ultrapure water and 1 mL Folin-Ciocalteu reagent. Then, the mixture reacted in the dark at 30 °C for 5 min. After that, 3.0 mL Na_2CO_3 (2 %) was added, and the mixture was incubated in darkness at room temperature for 2 h. Finally, the absorbance of the above solution was determined at 760 nm. The grafting ratio of CDOS-CA conjugates was expressed as mg of CA equivalent per g (mg CA/g) of the conjugates by using CA as a standard.

2.4.2. Structural properties

UV–vis spectra at 200 – 600 nm of CDOS-CA conjugates were determined using a U-3900 spectrophotometer (Hitachi, Japan). The FTIR spectra of CDOS-CA conjugates were determined by an FTIR spectrophotometer (Nicolet NEXUS, Thermo, USA) in the wavelength range from 4000 to 500 cm^{-1}. X-ray diffraction (XRD) pattern of CDOS-CA conjugates was obtained by an Axs D2 PHASER X-ray diffractometer (Bruker, Germany) in a 2θ range from 5° to 50° and the scanning speed was set at 2°/min.

2.4.3. Morphological properties

The surface morphology of CDOS-CA conjugates was visualized by a scanning electron microscope (SEM, FEI Quanta 200, FEI Company, Eindhoven, The Netherlands) at 10 kV accelerating voltage.

2.4.4. Thermal stability analysis

DSC analysis of CDOS-CA conjugates was performed using a DSC Q200 (TA Instruments, USA). The thermogravimetric analysis of CDOS-CA conjugates was investigated with a TGA2 automatic thermogravimetric analyzer (Toledo, Mettler, Switzerland).

2.5. In vitro simulated gastrointestinal digestion of CDOS-CA conjugates

The simulated gastrointestinal digestion of samples was performed as described previously (Xie et al., 2022). Following the digestion order, simulated gastric fluid (SGF), simulated intestinal fluid (SIF), and simulated colonic fluid (SCF) were sequentially added to the samples. In brief, sample solution (50 mL) was mixed with 50 mL of SGF containing porcine pepsin (2 mL, 6500 U/mL) at pH 1.2 for 2 h. After the reaction, SIF (100 mL) containing porcine pancreatin (20 mL, 800 U/mL) was added to the mixture and digested at pH 6.8 for 4 h. Finally, the same volume of SCF was added and the mixture was digested at pH 7.4 for 24 h. After digestion of SGF, SIF and SCF, the digested samples were collected to analyze their antioxidant activity and CA retention content.

The antioxidant activity of CDOS-CA during *in vitro* digestive process was determined by DPPH/ABTS free radical scavenging capacity (Xiao et al., 2022) and ferric ion reducing antioxidant power according to the previous studies (Zhang et al., 2023). Samples after SGF, SIF and SCF digestion were centrifuged at 8000 × *g* for 10 min at 4 °C, then the supernatants were used to determine the retained CA content using the Folin-Ciocalteu method according to Limwachiranon et al. (Limwachiranon et al., 2020).

2.6. In vitro human fecal fermentation

Samples after being digested in SGF for 2 h and then SIF for 4 h were lyophilized for colonic fermentation. The *in vitro* fecal fermentation of the digested samples was performed according to the previous methods with modifications (Li et al., 2022b). Fresh human feces were collected from 4 healthy volunteers (2 males and 2 females, 23–28 years of age) who did not take any antibiotics in the past three months or did not have gastrointestinal disease. Fecal slurry (10 %, m/v) was prepared through filtering the fecal mixture diluted with sterile PBS (pH 7.4) by a four-layer cotton gauge. The basal fermentation medium (1.0 L) consisted of glucose (2.0 g), yeast extract (3.0 g), tryptone (1.0 g), casein (2.0 g), L-cysteine (0.5 g), NaCl (0.5 g), KH_2PO_4 (0.5 g), K_2HPO_4 (0.5 g), $CaCl_2{\cdot}6H_2O$ (0.15 g), $MgSO_4{\cdot}7H_2O$ (0.01 g), hemin (0.025 g), bile salt (0.4 g), resazurin (1.0 mg), Tween 80 (1.0 mL), and vitamin K (2.0 mg). 50 mg fructooligosaccharide (FOS, FOS group), 50 mg CDOS (CDOS group), 50 mg CDOS-CA (CDOSCA group), and 10 mg CA (CA group) were added to the mixture of fresh human fecal slurry (1.0 mL) with 9.0 mL basal nutrient medium. The mixture of basal medium with fecal bacteria was used as the original microbial community (CK0H group) and as a blank group after incubating at 37 °C for 24 h (Control group).

2.7. Determination of SCFAs

The concentrations of SCFAs of each fermented group at the fermentation time of 24 h were determined as described in a previous study (Li et al., 2022d).

2.8. Microbial community analysis

Total microbial DNA was extracted from the bacteria in the fermentation medium by using the QIAamp DNA Stool Mini Kit (Qiagen, Hilden, Germany). The V3 – V4 region of the bacteria 16S rRNA amplified with the universal 515F/806R primers. Operational taxonomic units were obtained by Uparse (v7.0.1001) in accordance with the sequence similarity of 97 % and the sequencing data were analyzed using QIIME. Linear discriminant analysis effect size (LEfSe) analysis was performed to determine key genera of gut microbiota among different groups with a threshold more than 4.0.

2.9. Statistical analysis

All experiments were performed in triplicate and the values were reported as means ± standard deviations. Statistically significant differences were performed using SPSS Statistics 22.0 software and $p < 0.05$ presented the statistical significance of differences.

3. Results and discussion

3.1. Characterization of CDOS-CA conjugates

As obtained in SEC-MALLS analysis (Fig. 1A), the Mw of CD was determined to be 1312.69 kDa. Furthermore, MALDI-TOF mass spectrometry was employed to characterize the degree of polymerization (DP) of CDOS in the positive mode. Under those conditions, oligosaccharides were ionized preferentially as sodium adducts ($[M + Na]^+$) (Zhu, Chen, Chang, Qiu, & You, 2023). As shown in Fig. 1B, 4 peak groups represented oligomers of different lengths (*m/z* from 527 to 1013). The peak-to-peak mass difference of CDOS determined to be 162 Da, corresponding to the mass of one glucose unit ($C_6H_{10}O_5$, 162 Da) (Yu et al., 2016). According to the mass charge ratio of linear glucan: $m/z = 162 \times n\ (DP) + 18 + 23$ (Na, the cationization ion), it was clear that the CDOS with *m/z* 527.13, 671.17, 851.24, and 1013.31 corresponded to oligosaccharides with DP = 3, 4, 5, and 6, respectively (Zhu et al., 2023). The above results showed that water-soluble CDOS with a DP of 3–6 can be obtained from high molecular weight insoluble CD through H_2O_2 degradation. During the H_2O_2 degradation, active hydroxyl radicals (•OH) could react with CD by abstracting carbon-bound hydrogen atoms (C—H) to form free CD macro radicals. The abstraction of hydrogen from C-1 and C-3 could induce the cleavage of the β-1, 3-glycosidic bond of CD (Fig. 1E). The rearrangement of free carbohydrate fragment radicals and chain scission led to the decrease in the Mw of CD (Pan et al., 2013).

The UV–vis spectra of CD, CDOS, CDOS-CA, and CA displayed in Fig. 1C. CD and CDOS showed two peaks at 218 nm and 260 nm with similar profiles, although the peak intensity of CDOS was significantly higher than that of CD. Pan et al. also reported an increased peak intensity of around 260 nm in konjac glucomannan after H_2O_2 degradation ascribed to the formation of carbon–oxygen double bonds following the chain scission of the polysaccharide (Pan et al., 2013). CA presented two characteristic absorption peaks at approximately 303 nm and 332 nm, corresponding to the π-system of the benzene ring (Cai et al., 2019). A characteristic absorption peak of CA at 327 nm (Fig. 1C) was observed in the spectrum of CDOS-CA (Rui et al., 2017), suggesting the successful grafting of CA onto CDOS. Slight blue shifts in the peak at 327 nm of CDOS-CA in comparison with that of free CA could be attributed to the covalent linkages of CA with CDOS. Similar blue shift results were also found in ferulic acid-grafted curdlan conjugates (Cai et al., 2019). Furthermore, the peak of CDOS-CA conjugates at 281 nm, compared to the peak at 258 nm of CDOS, showed a redshift. This redshift was related to the reduced energy required for the π-π* transition caused by covalent grafting between CDOS and CA (Xiao et al., 2022). According to the Folin-Ciocalteu reagent assay, the grafting ratio of CDOD-CA conjugates prepared under an ultrasonication-assisted Fenton system was calculated to be 296.79 ± 19.59 mg CA/g polymer, which was much higher than that of gallic acid grafted inulin (16.3 mg/g polymer) (Arizmendi-Cotero, Villanueva-Carvajal, Gómez-Espinoza, Dublán-García, & Dominguez-Lopez, 2017). Ultrasound treatment could accelerate the free radical movement to improve the grafting efficiency of CA. In a previous study, the grafting ratio of efficiency of the chitosan-ferulic acid conjugate was enhanced by the ultrasonication-assisted Fenton system, which also reduced the degradation of the conjugates under the Fenton system (Xu et al., 2023).

The FTIR spectra of CD, CDOS, CDOS-CA, and CA were presented in Fig. 1D. The FTIR spectra of CD and CDOS were generally similar, exhibiting characteristic peaks around 3314 cm^{-1} (stretching vibrations of –OH), 2883 cm^{-1} (C—H stretching), 1156 cm^{-1} (β-(1 → 3) glucoside bonds), 1070 (C—O—H stretching vibrations) and 889 cm^{-1} (β-glycosidic bonds) (Cai et al., 2019). However, a new peak at 1597 cm^{-1} attributed to the asymmetrical symmetrical stretching of the COO^- group (Bai, Yong, Zhang, Liu, & Liu, 2020) was observed in CDOS. The hydroxy groups in the pyranose rings were first dehydrogenated and oxidized to form a carbonyl group, followed by ring opening to form a carboxyl group (Pan et al., 2013; Zhu et al., 2023). Qin et al. also found that the H_2O_2 degradation of β-glucan promoted the substitution of hydroxyl groups, resulting in the formation of carbonyl and carboxyl groups (Qin et al., 2021). CA exhibited typical phenolic characteristic peaks at 3324 cm^{-1} (O—H stretching of hydroxyl groups), 1687 cm^{-1} (C═O stretching vibration of a mixed ester and carboxyl groups), and 1638–1444 cm^{-1} (benzene ring stretching vibrations) (Luo et al., 2023). The FTIR spectrum of the CDOS-CA conjugates was more similar to that of CDOS than to the spectrum of CA. Notably, CDOS-CA conjugates exhibited typical C═C aromatic rings at 1599 cm^{-1} and 1518 cm^{-1},

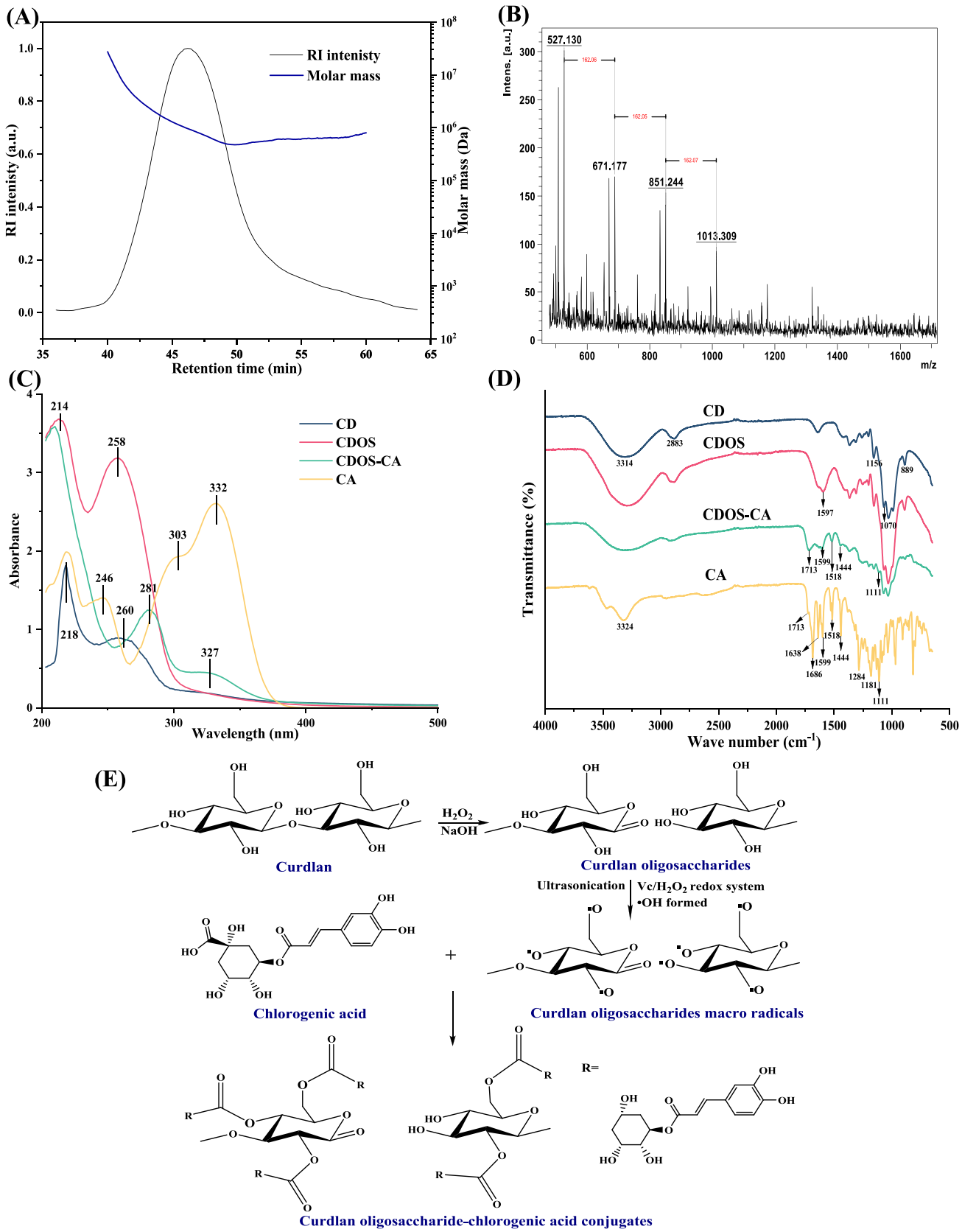

Fig.1. (A) SEC-MALLS chromatogram of curdlan (CD). (B) MALDI-TOF mass spectrometry analysis of curdlan oligosaccharides (CDOS). (C) The UV–vis spectra of CD, CDOS, CDOS-CA conjugates and chlorogenic acid (CA). (D) The FTIR spectra of CD, CDOS, CDOS-CA and CA. (E) The proposed mechanism for the synthesis of CDOS-CA under the ultrasonication-assisted Fenton-system.

carbonyl groups (C═O) at 1713 cm^{-1} (Xiao et al., 2022), and a series of characteristic peaks of CA. These results suggested that CA was efficiently grafted onto the CDOS molecular chains.

In this study, the CDOS was grafted with CA (CDOS-CA) using a free radical-mediated method under an ultrasonication-assisted Fenton system. The proposed mechanism for CA grafting onto CDOS was depicted in Fig. 1E. To improve the solubility and biological activity of CD, water-soluble CDOS was obtained by alkaline hydrolyzing CD with H_2O_2, leading to glycosidic bond hydrolysis and ring scissions (Ovalle, Chen, Soll, Moore, & Lipke, 2020). Subsequently, graft copolymerization CDOS with CA was initiated through Vc/H_2O_2 induced macro radicals in the CDOS chains (Cai et al., 2019). In the ultrasound-assisted Fenton system, Vc initially reacted with H_2O_2 to produce ascorbate and hydroxyl (•OH) radicals. These oxidation components attacked the susceptible group in the CDOS backbone, consequently generating radical species on the CDOS. Finally, the CA molecule accepted the CDOS radicals, forming a new CDOS-CA conjugate.

3.2. The crystallographic structure

The crystallographic structures of CD, CDOS, CDOS-CA, and CA were determined by XRD, and the results were shown in Fig. 2A. CD showed a small and a large broad peak at 2θ 10.07 and 20.03, respectively, indicating the semi-crystalline structures of CD attributed to the inter-/intramolecular hydrogen bonds and Van der Waals forces in polysaccharide network (Johnson, Lee, Jayabalan, & Suh, 2020). After H_2O_2 degradation, CDOS exhibited an amorphous state, indicating the breakdown of CD's crystalline structures. The amorphous structures of CDOS facilitated a high grafting rate by enhancing the interaction between the molecular fragments of CD and CA. CA showed several sharp diffraction peaks, indicating it was a crystalline compound, which was consistent with the regular needle-like morphology of CA observed by SEM (Fig. 3 d). However, the sharp peaks of CA were not observed in CDOS-CA. Furthermore, the main diffraction peak intensity of CDOS-CA decreased compared with CDOS due to the significant breakage of hydrogen bonds in CDOS after CA conjugation (Bai et al., 2020).

3.3. Micromorphology

The micromorphology of CD, CDOS, CDOS-CA, and CA was evaluated by SEM. As shown in Fig. 3A/a, CD exhibited an irregular block-like structure with diverse particle sizes and shapes, presenting a relatively rigid and smooth surface. After alkaline H_2O_2 treatment, CDOS presented a rod-like and sheet-like morphology. Additionally, when magnified at 5000 times (Fig. 3b), scale-like structures were observed on the surface of CDOS. A similar phenomenon was found in ginseng dietary fiber that alkaline H_2O_2 treatment led to a loosened inner structure and rougher surface (Jiang et al., 2021). The loosened structure of CDOS could be caused by the disruption of hydrogen bond dissociation between the triple helices of CD or the degradation of macromolecular chains (Pan et al., 2013). Especially, the morphology of CDOS was significantly changed after grafting with CA. CA was a regular needle-

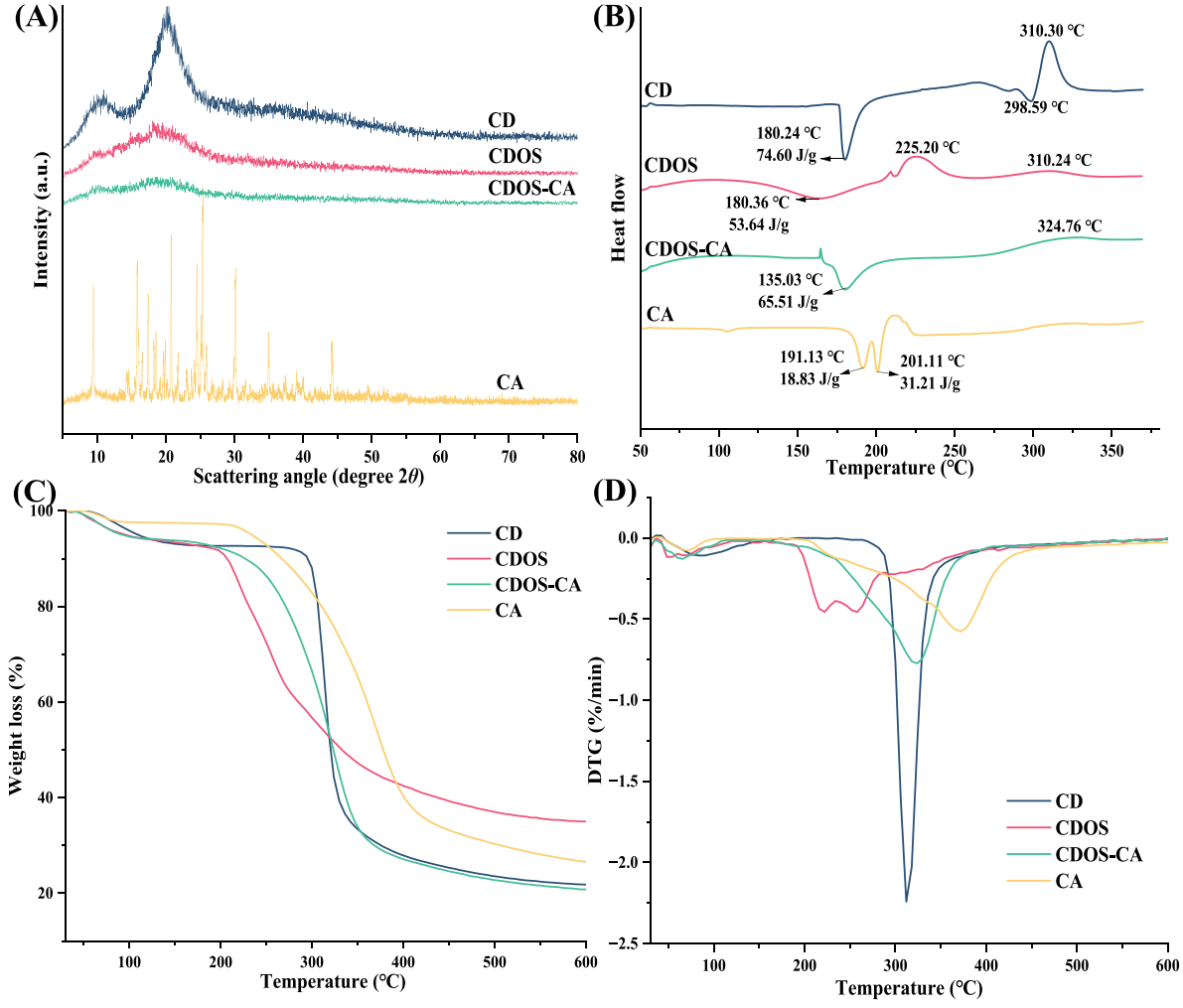

Fig.2. (A) X-Ray diffraction, (B) differential scanning calorimetry, (C) thermal gravimetric analysis and (D) derivative thermo gravimetric analysis of curdlan (CD), curdlan oligosaccharides (CDOS), CDOS-CA conjugates and chlorogenic acid (CA).

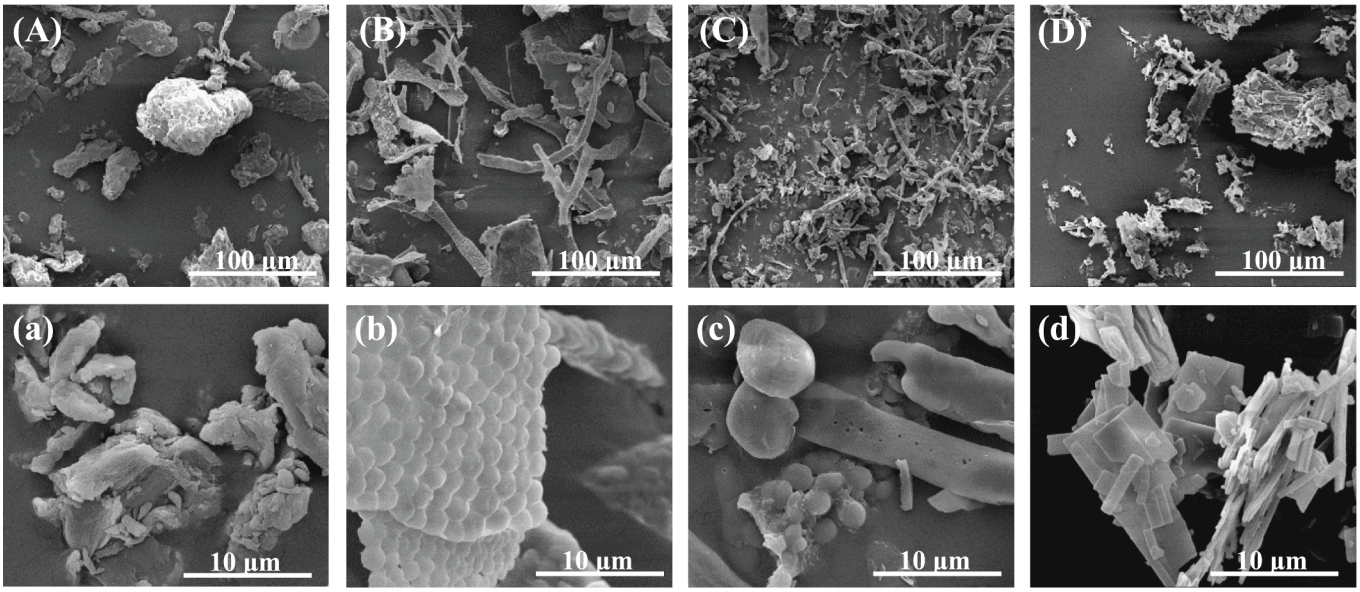

Fig.3. Scanning electron microscope images of (A/a) curdlan (CD), (B/b) curdlan oligosaccharides (CDOS), (C/c) CDOS-CA conjugates and (D/d) chlorogenic acid (CA) at 500/5000X.

like crystalline compound (Fig. 3D/d), whereas CDOS-CA presented several different shapes, such as sheet-like, rod-like, and round morphology. Moreover, the particle size of CDOS-CA was much smaller than that of CDOS. This result indicated that grafting CA resulted in a looser structure of CDOS. A similar phenomenon was found in gallic acid-grafted O-carboxymethyl chitosan (Bai et al., 2020) and ferulic acid-grafted carboxylic curdlan (Wang, Zhang, Qiao, Cai, & Yan, 2021).

3.4. Thermal properties of CDOS-CA conjugates

DSC was used to measure the occurrence of endothermic or exothermic changes during heating (Johnson et al., 2020). The DSC thermogram of native CD, CDOS, and CDOS-CA conjugate showed much distinct difference (Fig. 2B). Native CD exhibited two endothermal changes at 180.24 °C and 298.59 °C, and an exothermal change at 310.30 °C. CDOS showed a broad endothermic peak at 135.03 °C, and a small and a broad exothermic peak at 225.20 °C and 310.24 °C, respectively, indicating decreased thermal stability of CD after oxidative degradation. Additionally, the melting enthalpy (ΔH) value of CDOS (65.51 J/g) in the first endothermic change was lower than that of CD (74.60 J/g), which further confirmed the reduced thermal stability of CDOS. The decreased endothermic transition temperature corresponded to the weakening of inter-/intra-molecular hydrogen interactions, the reduction of Mw, and the disruption of the rigid triple helical structure in CD (Yan et al., 2020). This result was correlated with the SEM observation that the CDOS was more loosely structured than the CD. Compared with CDOS, CDOS-CA conjugate exhibited an evident endothermic peak at 180.36 °C, and an exothermic peak at 324.76 °C, indicating the thermal stability of CDOS increased after grafting with CA. The DSC profile of the CA exhibited endothermic peaks at 191.13 – 201.11 °C, representing the melting temperature of CA. However, the CA characteristic peak disappeared in CDOS-CA, providing evidence for the grafting of CA onto CDOS molecular.

TGA was used to investigate the thermal stability, thermal degradation, and weight loss of material during heating (Luo et al., 2023). The TGA and derivative thermo gravimetric (DTG) curves for CD, CDOS, CDOS-CA, and CA were shown in Fig. 2C–D. The weight loss of the samples mainly occurred at 50 – 600 °C, which presented a three-stage thermal degradation trace: 50 – 150 °C, 150 – 400 °C, and 400 – 600 °C. The first stage of weight loss was attributed to the loss of water, where only about 2 % weight loss rate in CA and 6 % in other samples. In the second stage, the rapid weight loss was caused by the degradation of the samples, and the initial degradation temperature for CD, CDOS, CDOS-CA, and CA was about 291 °C, 198 °C, 243 °C, and 264 °C, respectively. The weight loss at the third stage (400 – 600 °C) was slow, and the residue weight of CD, CDOS, CDOS-CA, and CA was 21.81 %, 35.00 %, 20.80 %, and 26.55 %, respectively. Those results demonstrated higher thermal stability for CD compared to CDOS, while the intercalation of CA into CDOS increased the decomposition temperature of CDOS-CA conjugates. The DTG results indicated the maximum decomposition rates of CD, CDOS, CDOS-CA and CA appeared at 312 °C, 221/256 °C, 322 °C, and 371 °C (Fig. 2D), respectively. It was consistent with the DSC results that oxidative degradation reduced the thermal stability of CD but grafting CA onto CDOS improved the thermal stability of CDOS.

3.5. In vitro simulated digestion of CDOS-CA conjugate

Excess free radicals generated from the oxidation of protein, lipids, and sugar can lead to high levels of oxidative stress, which would exhibit negative impacts on human health (Li et al., 2021). As shown in Fig. 4A, in undigested samples (BD), there was no significant difference in DPPH/ABTS scavenging ability between CD and CDOS ($p > 0.05$), but CDOS (11.12 mg $FeSO_4$/g) presented a much higher ferrous reducing power than CD (1.16 mg $FeSO_4$/g). The hydroxyl exposure and reduction of intermolecular hydrogen bonds during oxidative degradation can promote the transfer of hydrogen from low molecular weight CDOS molecules under physiological conditions, resulting in a high antioxidant capacity (Luo et al., 2023). The DPPH/ABTS scavenging ability of CDOS-CA conjugates (51.04 % DPPH scavenging ability and 90.20 % ABTS scavenging ability in BD) was significantly higher than that of CDOS (only 0.65 % DPPH scavenging ability and 0.58 % ABTS scavenging ability in BD), demonstrating that the insertion of CA into the CDOS chain can enhance the DPPH/ABTS scavenging ability. Furthermore, both the ABTS scavenging ability and ferrous reducing power of CDOS-CA were significantly higher than that of CA (same concentration as the CA content in CDOS-CA). The above results suggested that CA not only retained its excellent antioxidant ability but also synergistically exerted antioxidant ability after grafting with CDOS. The water solubility of CA can be improved by grafting with CDOS, thereby CDOS-CA exhibited a prominent ability to scavenge free radicals due to the increased H-atom donors (Xiao et al., 2022). Rui et al also found that enhanced antioxidant activity of CA-soluble oat β-glucan conjugates due

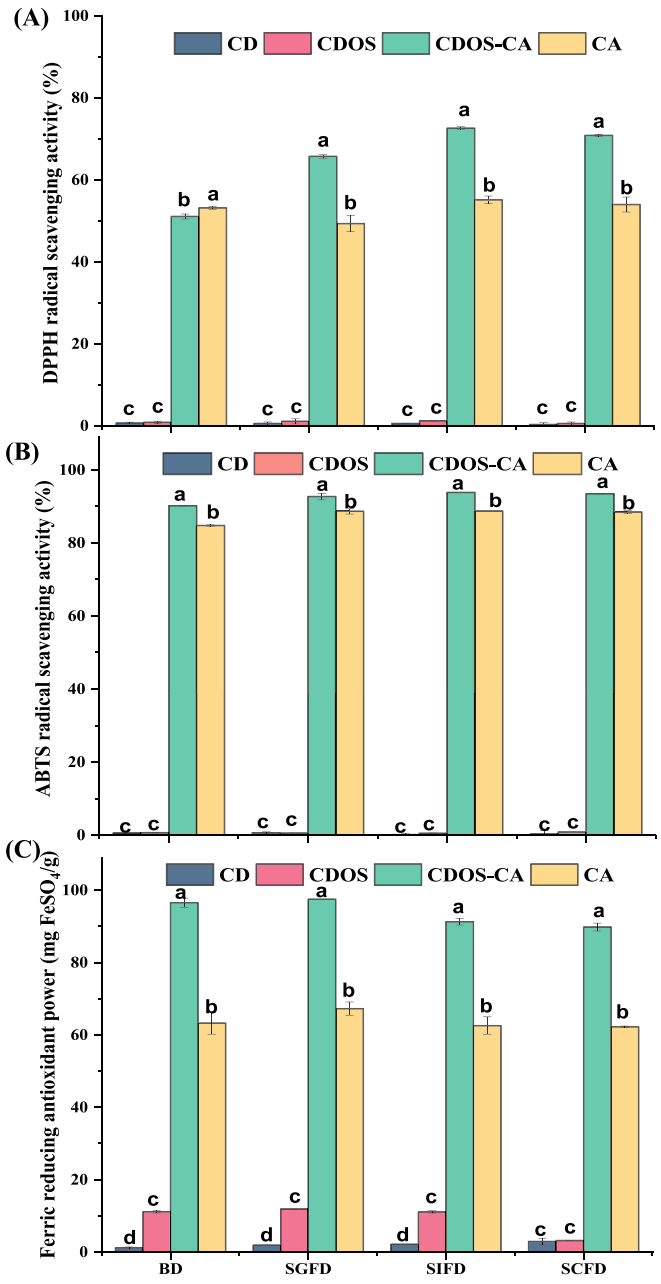

Fig. 4. (A) DPPH radical scavenging activity, (B) ABTS radical scavenging activity, and (C) Ferric reducing antioxidant power of curdlan (CD), curdlan oligosaccharides (CDOS), CDOS-CA conjugates and chlorogenic acid (CA) during *in vitro* digestion. Note: BD stands for undigested samples; SGFD represents the sample after digestion of simulated gastric fluid; SIFD represents the sample after digestion of simulated intestinal fluid; SCFD represents the sample after digestion of simulated colonic fluid; Different letters represent significant differences between different samples after the same digestion treatment ($p < 0.05$).

to the grafting oat β-glucan with CA (Luo et al., 2023).

After digestion of simulated gastric acid for 2 h (SGFD), simulated small intestine for 4 h (SIFD), and simulated colon for 24 h (SCFD), the antioxidant activity of CDOS-CA was shown in Fig. 4. According to the ABTS/DPPH antioxidant assay, a slight increase in the antioxidant activity of CDOS-CA (in SGFD, SIFD, and SCFD) was observed after digestion, possibly due to the hydrolysis of CA into small molecular phenolic acids with higher antioxidant activity. In SGFD, the ability of CA to scavenge water-soluble ABTS radicals increased from 84.75 % to 88.64 % after gastric acid digestion, while the ability to scavenge alcohol-soluble DPPH radicals decreased from 53.14 % to 49.30 %. These two opposite trends could be attributed to the fact that the molecular structure of CA was destroyed after gastric acid digestion, leading to a decreased DPPH scavenging ability, whereas the increased water-solubility of CA after digestion led to an increased ABTS scavenging ability. After three stages of digestion, the ferric reducing capacity of CDOS-CA was decreased from 96.56 % to 89.83 %, and that of CA from 63.34 % to 62.24 %. The antioxidant capacity of CDOS-CA and CA determined by different assays showed different trends during digestion, which may be related to the disrupted molecular structure and increased water solubility of the samples during the digestion process. During digestion, the antioxidant capacity of CDOS-CA was much higher than that of CA, suggesting that CDOS-CA could provide a favorable antioxidant environment in the digestive tract.

After the three stages of digestion, 91.65 % of the CA content in CDOS-CA was retained, whereas the CA content in the free CA samples increased by 4.46 % in SGFD, but decreased by 32.75 % and 43.27 % in SIFD and SCFD, respectively (Fig. S1). The complex formed between CA and CDOS may have prevented direct contact of pepsin with CA, leading to higher retention of CA. In addition, CA was relatively stable in acidic conditions, which resulted in less damage to CA under gastric acid conditions and more loss in small intestinal fluid and colonic fluid environments. This phenomenon indicated that CDOS could improve the digestive stability of CA, and a similar result was found in CA-amylopectin complex (Limwachiranon et al., 2020). In conclusion, CDOS-CA showed excellent antioxidant capacity in the digestive tract with good gastrointestinal stability, which exhibited the potential to relieve intestinal oxidative stress and can be used as an antioxidant supplement to improve intestinal health.

3.6. SCFA analysis

The content of SCFAs, including acetic acid, propionic acid, butyric acid, valeric acid, isobutyric acid, and isovaleric acid, as well as pH value after 24 h of *in vitro* fecal fermentation, were presented in Table 1. Acetic acid, propionic acid, and butyric acid made up the majority of the total SCFAs, which was in good agreement with the results in the fermentation of mung bean coat polyphenols (Xie et al., 2022). Compared with the CDOS and CA groups, the CDOS-CA group showed larger production of propionic acid (10.81 mM), butyric acid (9.08 mM) and total SCFAs (31.82 mM), which was positively related with the higher abundance of *Prevotella* in CDOS-CA group (Fig. 5B). This was similar to the result that CDOS-CA exhibited higher antioxidant activity than CDOS and CA, which suggested a possible synergistic effect with CDOS and CA. Arizmendi-Cotero et al. also found that grafting gallic acid onto the backbone of inulin gave to the new polymer significant antioxidant and probiotic capacities (Arizmendi-Cotero et al., 2017). However, there was no significant difference in the content of SCFAs between CDOS and CA groups, while the composition of gut microbiota was obviously different. CDOS could specifically enrich probiotics of *Faecalibacterium* and *Megamonas*, but CA could specifically enrich *prevotella* and *Dialister* (*Fig. S2*). Probiotics that metabolize both carbohydrates (eg. CDOS) and phenolic acids (eg. CA) could promote the production of SCFAs, which may lead to a less pronounced SCFAs difference between the CDOS and CA groups. FOS was chosen as the positive control because of its well-known prebiotic property (Li et al., 2022a). The content of butyric acid in CDOS-CA group (9.08 mM) was significantly higher than that in FOS group (1.49 mM). Among all SCFAs, butyric acid is a key regulator in the metabolic control of the microbiota, and up to 95 % of butyric acid can be consumed in the colon (Li et al., 2023). Butyric acid could maintain the integrity of the intestinal barrier, regulate inflammatory responses and relieve oxidative stress (Xie et al., 2022), which was an important prebiosis marker.

Furthermore, the total SCFA content of the CDOS-CA group was significantly higher than those of the CDOS and CA groups ($p < 0.05$), suggesting a synergistic effect between CDOS and CA in terms of

Table 1
The individual and total SCFAs content as well as pH values after *in vitro* fermentation of CDOS-CA conjugates.

Sample	Acetic acid (mM)	Propionic acid (mM)	Butyric acid (mM)	Valeric acid (mM)	Isobutyric acid (mM)	Isovaleric acid (mM)	Total SCFAs (mM)	pH value
Control	10.24 ± 1.89^{b}	8.41 ± 0.42^{bc}	1.18 ± 0.21^{c}	1.40 ± 0.02^{a}	0.19 ± 0.01^{a}	0.44 ± 0.03^{a}	21.86 ± 2.58^{c}	5.82 ± 0.05^{a}
FOS	15.44 ± 1.59^{a}	9.38 ± 0.39^{b}	1.49 ± 0.20^{c}	1.45 ± 0.47^{a}	0.09 ± 0.02^{a}	0.11 ± 0.19^{b}	27.96 ± 2.86^{ab}	4.20 ± 0.04^{e}
CDOS	9.93 ± 1.96^{b}	7.69 ± 0.43^{cd}	5.57 ± 0.34^{b}	0.68 ± 0.15^{b}	0.14 ± 0.06^{a}	0.01 ± 0.01^{b}	24.02 ± 2.95^{bc}	4.75 ± 0.03^{c}
CDOS-CA	11.06 ± 0.29^{b}	10.81 ± 0.63^{a}	9.08 ± 0.39^{a}	0.69 ± 0.11^{b}	0.08 ± 0.01^{a}	0.10 ± 0.01^{b}	31.82 ± 1.44^{a}	4.33 ± 0.03^{d}
CA	9.05 ± 0.41^{b}	7.15 ± 0.76^{d}	5.39 ± 1.09^{b}	0.80 ± 0.23^{b}	0.08 ± 0.03^{a}	0.08 ± 0.03^{b}	22.55 ± 2.75^{c}	5.00 ± 0.04^{b}

All experiments were performed in triplicate and values were presented as mean ± SD. Different letters mean significant differences ($p < 0.05$) in the same column.

prebiotic activity. Therefore, the prebiotic activity of CDOS-CA could be enhanced through grafting CA. Compared with straight-chain fatty acids, the content of branched-chain fatty acids (isobutyrate and isovalerate) was much lower, which was related to the risks of colon cancer (Zhao et al., 2021). The branched-chain fatty acids contents in the CDOS-CA group were significantly lower compared to the Control group. The decreased isobutyrate/isovalerate levels were beneficial for the host's health. In conclusion, CDOS-CA could be utilized by gut microbes to promote the synthesis of beneficial SCFAs, especially butyric acid production, while reducing the production of harmful branched-chain fatty acids, potentially contributing to colonic health.

3.7. Gut microbial composition

The composition of gut microbiota was characterized by analyzing the structural differences in each group (Fig. 5). At the phylum level (Fig. 5A), compared with the Control group (12.50 %), a decrease of Proteobacteria (a hallmark of intestinal microecological disorders) was observed in the CDOS (5.73 %), CDOSCA (5.24 %), and CA (7.79 %) groups, indicating CDOS or CDOS-CA supplement could inhibit the growth of Proteobacteria.

At the genus level (Fig. 5B), *Bacteroides* were the most dominant genus in all the tested groups (25.87–38.64 %). *Bacteroides* were considered to be a new type of probiotic that can secrete glycosidase to degrade dietary carbohydrates, produce SCFAs, and maintain intestinal homeostasis (Ji et al., 2021; Xie et al., 2022). Compared with the Control group, the relative abundances of beneficial gut microbiota *Prevotella* and *Faecalibacterium* in the CDOS and CDOS-CA intervention groups increased significantly ($p < 0.05$), whereas pathogenic bacteria *Klebsiella*, *Escherichia-Shigella*, and *Alistipes* showed a decreased trend. *Prevotella* genus were versatile saccharolytic microorganisms associated with plant-rich diets, which exhibited high capacity in digestion and fermentation of polysaccharides (Liu, Chen, Zhang, & Ni, 2022). *Faecalibacterium* genus is butyrate-producing bacteria, whereas *Escherichia-Shigella* is a common pathogenic bacteria considered to be strongly associated with the imbalance of gut microbiota and even chronic colitis (Feng et al., 2023). β-glucan in the CDOS and CDOS-CA molecular chains can be fermented by those beneficial microbiota to produce SCFAs to achieve the hypocholesterolemic as well as maintain blood glucose homeostasis (Chen, Huang, Wang, Geng, & Nie, 2022). In particular, the abundance of beneficial bacteria *Prevotella*, *Lactobacillus,* and *Bifidobacterium* increased after fermentation of CDOS-CA compared with that of CDOS, indicating that CA grafting could improve the probiotic activity of CDOS. Previous study also reported that CA can promote the growth of *Bifidobacteria* and can be metabolized into easily absorbed small phenolic acids to modulate intestinal inflammation (Zeng, Xiang, Fu, Qu, & Liu, 2022). The proliferation of *Prevotella* in the CDOS-CA group could be helpful to regulate blood glucose, thereby reducing the risk of developing diabetes (Feng et al., 2023). Liu et al. also reported that the administration of green tea phenolics could increase the abundance of *Prevotella* (Liu et al., 2022). Therefore, grafting CA can improve the probiotic activity of CDOS. CDOS-CA conjugate was decomposed by the gut microbiota into oligosaccharides and free small phenolic acids with higher biological activity, and these components have synergistic effects in modulating the gut microbiota (Li et al., 2022d).

The weighted UniFrac principal coordinate analysis (PCOA) was performed to analyze the β diversity of different groups. As demonstrated in Fig. 5C, PC1, and PC2 contributed 53.11 % and 19.11 % of the variation, respectively, suggesting that the community of gut microbiota was significantly influenced by different fermentation substrates. The PCOA plot showed that Control groups without supplements presented a distinct microbiota composition that clustered separately from CDOS and CDOS-CA groups, whereas the microbiota composition cluster of CDOS or CDOS-CA groups was relatively similar to the FOS group.

LEfSe analysis was performed to identify the significant abundance differences of species between the FOS, CDOS, CDOS-CA, and CA groups. As shown in Fig. 5D, 37 bacterial clades presented statistically significant differences, and 11, 3, 4, and 5 features were identified in the FOS, CDOS, CDOS-CA, and CA, respectively. It was noteworthy that the genus of *Klebsiella*, *Escherichia-Shigella*, and *Alistipes* belonged to the Proteobacteria and was found in the Control group, whereas those harmful bacteria disappeared after the intervention of FOS, CDOS, and CDOS-CA fermentation. Therefore, those supplementations could regulate the gut microbiota by inhibiting the growth of harmful microbiota. However, different supplements can specifically enrich various gut microbiota. The CDOS group contained a preponderance of the genera *Megamonas*, and the CA group was featured in the genera *Prevotella*. The CDOS-CA group was predominant with *Prevotella* and *Lactobacillaceae* (Fig. 5E). In a word, CDOS-CA conjugates ameliorated the human gut microbiota by elevating the abundance of probiotics that produced butyric acid and SCFAs. Therefore, CDOS-CA can be considered as promising nutraceuticals for modulating gut microbiota and improving oxidative stress.

4. Conclusions

CDOS with DP = 3–6 can be obtained by the H_2O_2 degradation of CD. The semi-crystalline structures of CD were dramatically broken down during oxidative degradation. UV–vis and FTIR spectra indicated that CDOS-CA conjugate was successfully synthesized by a free radical-mediated method. The amorphous state structures of CDOS facilitated the interaction between the molecular fragments of CD and CA, thereby improving the grafting efficiency. Grafting CA onto CDOS enhanced the thermal stability and antioxidant ability of CDOS. Moreover, CDOS-CA could maintain its antioxidant activity during *in vitro* digestion. It can be utilized by gut microbiota to improve the abundance of probiotics, inhibit harmful microbiota, and promote the synthesis of SCFAs, particularly butyric acid, contributing to colonic health. The CDOS-CA conjugates that existed good gastrointestinal stability, as well as

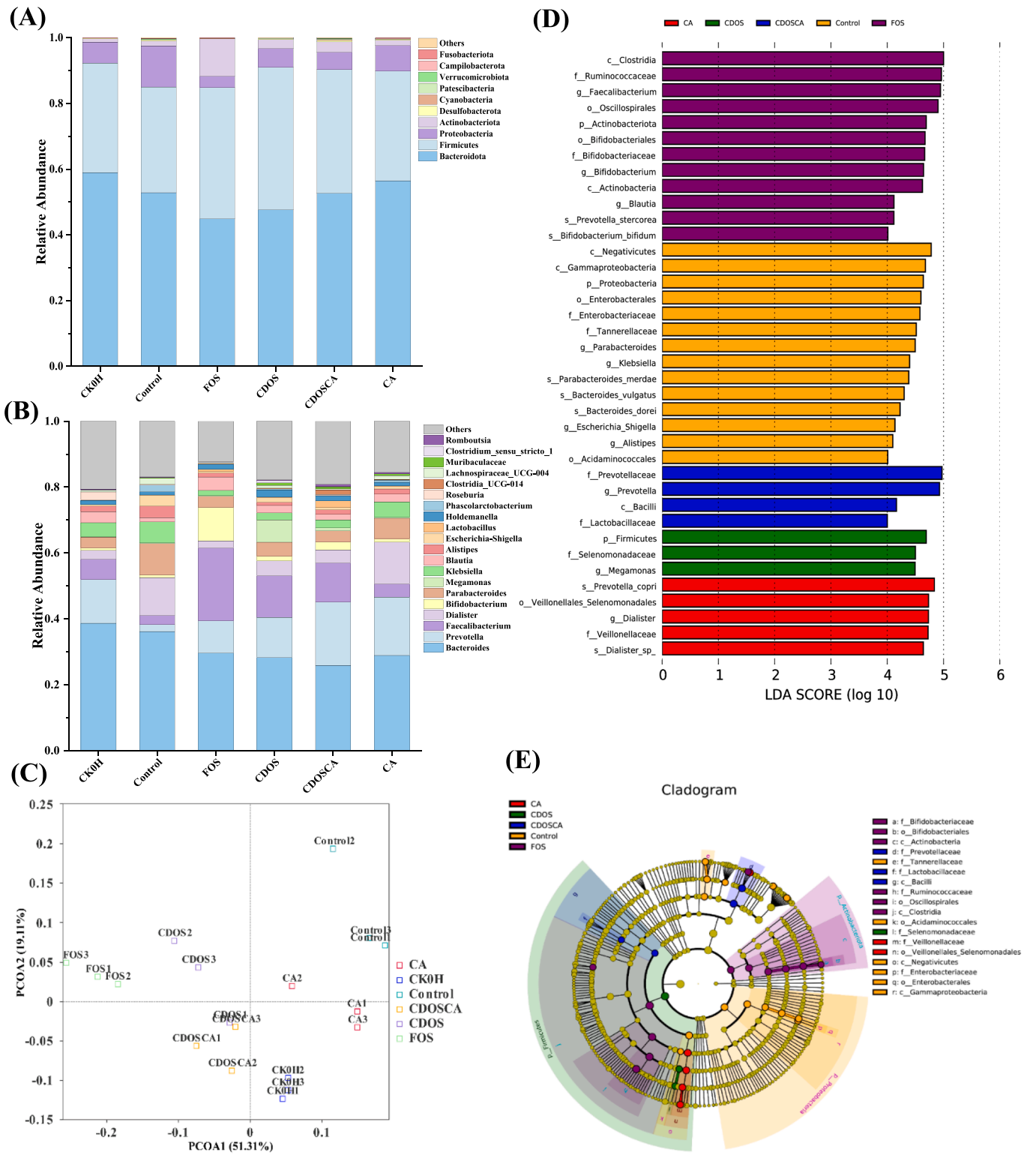

Fig. 5. Effects of CDOS, CDOS-CA and CA on gut microbial composition (A) at phylum level and (B) at genus level (n = 3 per group). (C) Principal coordinate analysis (PCOA) score plot based on unweighted-unifrac metrics of gut microbiota. (D) LEfSe analysis was performed to determine key genera of gut microbiota among different groups. (E) Cladogram depicting the LEfSe analysis' output.

antioxidant and probiotic activities can be used as a potential antioxidant dietary fiber or prebiotics in food and biomedical industries.

CRediT authorship contribution statement

Huan Li: Writing – review & editing, Writing – original draft, Methodology, Conceptualization. **Wenjiang He:** Supervision, Resources, Investigation. **Saiqing Xu:** Methodology, Data curation. **Rongrong Wang:** Resources, Conceptualization. **Shuai Ge:** Methodology, Investigation. **Haishan Xu:** Methodology, Investigation. **Yang Shan:** Supervision, Investigation. **Shenghua Ding:** Writing – review & editing, Supervision, Investigation, Funding acquisition.

Declaration of competing interest

The authors declare that they have no known competing financial interests or personal relationships that could have appeared to influence the work reported in this paper.

Data availability

Data will be made available on request.

Acknowledgements

This research was funded by The 14th Five-Year National Key Research and Development Plan Project (2023YFD2100300), National Natural Science Foundation of China (32272257), Natural Science Foundation of Hunan Province (2022JJ30330), Training Program for Excellent Young Innovators of Changsha (KQ1905025), the Agricultural Science and Technology Innovation Project of Hunan Province, China (2022CX44, 2022CX87), and Study on Strategy of Green Storage and High Value Utilization of Fruits and Vegetables (2023-XY-25).

Appendix A. Supplementary data

Supplementary data to this article can be found online at https://doi.org/10.1016/j.fochx.2023.101075.

References

Arizmendi-Cotero, D., Villanueva-Carvajal, A., Gómez-Espinoza, R. M., Dublán-García, O., & Dominguez-Lopez, A. (2017). Radical scavenging activity of an inulin-gallic acid graft and its prebiotic effect on *Lactobacillus acidophilus in vitro* growth. *Journal of Functional Foods, 29*, 135–142. https://doi.org/10.1016/j.jff.2016.12.014

Bai, R., Yong, H., Zhang, X., Liu, J., & Liu, J. (2020). Structural characterization and protective effect of gallic acid grafted O-carboxymethyl chitosan against hydrogen peroxide-induced oxidative damage. *International Journal of Biological Macromolecules, 143*, 49–59. https://doi.org/10.1016/j.ijbiomac.2019.12.037

Cai, W., Zhu, J., Wu, L., Qiao, Z., Li, L., & Yan, J. (2019). Preparation, characterization, rheological and antioxidant properties of ferulic acid-grafted curdlan conjugates. *Food Chemistry, 300*, Article 125221. https://doi.org/10.1016/j.foodchem.2019.125221

Chen, C., Huang, X., Wang, H., Geng, F., & Nie, S. (2022). Effect of β-glucan on metabolic diseases: A review from the gut microbiota perspective. *Current Opinion in Food Science, 47*, Article 100907. https://doi.org/10.1016/j.cofs.2022.100907

Feng, J., Wang, J., Bu, T., Ge, Z., Yang, K., Sun, P., et al. (2023). Structural, *in vitro* digestion, and fermentation characteristics of lotus leaf flavonoids. *Food Chemistry, 406*, Article 135007. https://doi.org/10.1016/j.foodchem.2022.135007

Grandpierre, C., Janssen, H. G., Laroche, C., Michaud, P., & Warrand, J. (2008). Enzymatic and chemical degradation of curdlan targeting the production of β-(1→3) oligoglucans. *Carbohydrate Polymers, 71*(2), 277–286. https://doi.org/10.1016/j.carbpol.2007.05.042

Ji, X., Zhu, L., Chang, K., Zhang, R., Chen, Y., Yin, H., et al. (2021). Chitooligosaccahrides: Digestion characterization and effect of the degree of polymerization on gut microorganisms to manage the metabolome functional diversity *in vitro*. *Carbohydrate Polymers, 275*, Article 118716. https://doi.org/10.1016/j.carbpol.2021.118716

Jiang, G., Bai, X., Wu, Z., Li, S., Zhao, C., & Ramachandraiah, K. (2021). Modification of ginseng insoluble dietary fiber through alkaline hydrogen peroxide treatment and its impact on structure, physicochemical and functional properties. *LWT - Food Science and Technology, 150*, Article 111956. https://doi.org/10.1016/j.lwt.2021.111956

Johnson, E. M. E., Lee, H., Jayabalan, R., & Suh, J.-W. (2020). Ferulic acid grafted self-assembled fructo-oligosaccharide micro particle for targeted delivery to colon. *Carbohydrate Polymers, 247*, Article 116550. https://doi.org/10.1016/j.carbpol.2020.116550

Li, M., Yang, R., Feng, X., Fan, X., Liu, Y., Xu, X., et al. (2022c). Effects of low-frequency and high-intensity ultrasonic treatment combined with curdlan gels on the thermal gelling properties and structural properties of soy protein isolate. *Food Hydrocolloids, 127*, Article 107506. https://doi.org/10.1016/j.foodhyd.2022.107506

Li, X., Chen, W., Gao, J., Gao, W., Zhang, Y., Zeng, H., et al. (2023). Structural changes of butyrylated lotus seed starch and its impact on the gut microbiota of rat *in vitro* fermentation. *Food Hydrocolloids, 139*, Article 108501. https://doi.org/10.1016/j.foodhyd.2023.108501

Li, D., Yao, X., Yang, Y., Cao, G., & Yi, G. (2022a). *In vitro* digestibility and fermentability profiles of wheat starch modified by chlorogenic acid. *International Journal of Biological Macromolecules, 215*, 92–101. https://doi.org/10.1016/j.ijbiomac.2022.06.083

Li, H., Gao, Z., Xu, J., Sun, W., Wu, J., Zhu, L., et al. (2022d). Encapsulation of polyphenols in pH-responsive micelles self-assembled from octenyl-succinylated curdlan oligosaccharide and its effect on the gut microbiota. *Colloids and Surfaces B: Biointerfaces, 219*, Article 112857. https://doi.org/10.1016/j.colsurfb.2022.112857

Li, M., Han, J., Xue, Y., Dai, Y., Liu, J., Gan, L., et al. (2019). Hydrogen peroxide pretreatment efficiently assisting enzymatic hydrolysis of chitosan at high concentration for chitooligosaccharides. *Polymer Degradation and Stability, 164*, 177–186. https://doi.org/10.1016/j.polymdegradstab.2019.04.011

Li, Y., He, D., Li, B., Lund, M. N., Xing, Y., Wang, Y., et al. (2021). Engineering polyphenols with biological functions via polyphenol-protein interactions as additives for functional foods. *Trends in Food Science & Technology, 110*, 470–482. https://doi.org/10.1016/j.tifs.2021.02.009

Li, Y., Luo, Y., Meng, F., Li, J., Chen, W., Liu, D., et al. (2022b). Preparation and characterization of feruloylated oat β-glucan with antioxidant activity and colon-targeted delivery. *Carbohydrate Polymers, 279*, Article 119002. https://doi.org/10.1016/j.carbpol.2021.119002

Limwachiranon, J., Huang, H., Li, L., Lin, X., Zou, L., Liu, J., et al. (2020). Enhancing stability and bioaccessibility of chlorogenic acid using complexation with amylopectin: A comprehensive evaluation of complex formation, properties, and characteristics. *Food Chemistry, 311*, Article 125879. https://doi.org/10.1016/j.foodchem.2019.125879

Liu, Z., Chen, Q., Zhang, C., & Ni, L. (2022). Comparative study of the anti-obesity and gut microbiota modulation effects of green tea phenolics and their oxidation products in high-fat-induced obese mice. *Food Chemistry, 367*, Article 130735. https://doi.org/10.1016/j.foodchem.2021.130735

Liu, N., Zou, S., Xie, C., Meng, Y., & Xu, X. (2023). Effect of the β-glucan from Lentinus edodes on colitis-associated colorectal cancer and gut microbiota. *Carbohydrate Polymers, 316*, Article 121069. https://doi.org/10.1016/j.carbpol.2023.121069

Luo, Y., Li, Y. C., Meng, F. B., Wang, Z. W., Liu, D. Y., Chen, W. J., et al. (2023). Simultaneously enhanced stability and biological activities of chlorogenic acid by covalent grafting with soluble oat β-glucan. *Food Chemistry: X, 17*, Article 100546. https://doi.org/10.1016/j.fochx.2022.100546

Ovalle, R., Chen, L., Soll, C. E., Moore, C. W., & Lipke, P. N. (2020). Regioselective degradation of [beta] 1,3 glucan by ferrous ion and hydrogen peroxide (Fenton oxidation). *Carbohydrate Research, 497*, Article 108124. https://doi.org/10.1016/j.carres.2020.108124

Pan, T., Peng, S., Xu, Z., Xiong, B., Wen, C., Yao, M., et al. (2013). Synergetic degradation of konjac glucomannan by gamma-ray irradiation and hydrogen peroxide. *Carbohydrate Polymers, 93*(2), 761–767. https://doi.org/10.1016/j.carbpol.2012.11.075

Qin, Y., Xie, J., Xue, B., Li, X., Gan, J., Zhu, T., et al. (2021). Effect of acid and oxidative degradation on the structural, rheological, and physiological properties of oat β-glucan. *Food Hydrocolloids, 112*, Article 106284. https://doi.org/10.1016/j.foodhyd.2020.106284

Rui, L., Xie, M., Hu, B., Zhou, L., Saeeduddin, M., & Zeng, X. (2017). Enhanced solubility and antioxidant activity of chlorogenic acid-chitosan conjugates due to the conjugation of chitosan with chlorogenic acid. *Carbohydrate Polymers, 170*, 206–216. https://doi.org/10.1016/j.carbpol.2017.04.076

Shi, Y., Liu, J., Yan, Q., You, X., Yang, S., & Jiang, Z. (2018). In vitro digestibility and prebiotic potential of curdlan (1→3)-β-D-glucan oligosaccharides in Lactobacillus species. *Carbohydrate Polymers, 188*, 17–26. https://doi.org/10.1016/j.carbpol.2018.01.085

Verma, D. K., Niamah, A. K., Patel, A. R., Thakur, M., Singh Sandhu, K., Chávez-González, M. L., et al. (2020). Chemistry and microbial sources of curdlan with potential application and safety regulations as prebiotic in food and health. *Food Research International, 133*, Article 109136. https://doi.org/10.1016/j.foodres.2020.109136

Wan, F., Cai, X., Wang, M., Chen, L., Zhong, R., Liu, L., et al. (2021). Chlorogenic acid supplementation alleviates dextran sulfate sodium (DSS)-induced colitis via inhibiting inflammatory responses and oxidative stress, improving gut barrier integrity and Nrf-2/HO-1 pathway. *Journal of Functional Foods, 87*, Article 104808. https://doi.org/10.1016/j.jff.2021.104808

Wang, Z., Zhang, Z., Qiao, Z., Cai, W., & Yan, J. (2021). Construction and characterization of antioxidative ferulic acid-grafted carboxylic curdlan conjugates and their contributions on β-carotene storage stability. *Food Chemistry, 349*, Article 129166. https://doi.org/10.1016/j.foodchem.2021.129166

Watanabe, K., Yamano, M., Masujima, Y., Ohue-Kitano, R., & Kimura, I. (2021). Curdlan intake changes gut microbial composition, short-chain fatty acid production, and bile acid transformation in mice. *Biochemistry and Biophysics Reports, 27*, Article 101095. https://doi.org/10.1016/j.bbrep.2021.101095

Xiao, X., Qiao, J., Wang, J., Kang, J., He, L., Li, J., et al. (2022). Grafted ferulic acid dose-dependently enhanced the apparent viscosity and antioxidant activities of arabinoxylan. *Food Hydrocolloids, 128*, Article 107557. https://doi.org/10.1016/j.foodhyd.2022.107557

Xie, J., Sun, N., Huang, H., Xie, J., Chen, Y., Hu, X., et al. (2022). Catabolism of polyphenols released from mung bean coat and its effects on gut microbiota during *in vitro* simulated digestion and colonic fermentation. *Food Chemistry, 396*, Article 133719. https://doi.org/10.1016/j.foodchem.2022.133719

Xu, H., Fu, X., Kong, H., Chen, F., Chang, X., Ding, Z., et al. (2023). Ultrasonication significantly enhances grafting efficiency of chitosan-ferulic acid conjugate and improves its film properties under Fenton system. *Food Research International, 164*, Article 112327. https://doi.org/10.1016/j.foodres.2022.112327

Yan, J., Cai, W., Wang, C., Yu, Y., Zhang, H., Yang, Y., et al. (2020). Macromolecular behavior, structural characteristics and rheological properties of alkali-neutralization curdlan at different concentrations. *Food Hydrocolloids, 105*, Article 105785. https://doi.org/10.1016/j.foodhyd.2020.105785

Yu, Y., Wang, Q., Yuan, J., Fan, X., Wang, P., & Cui, L. (2016). Hydrophobic modification of cotton fabric with octadecylamine via laccase/TEMPO mediated grafting.

Carbohydrate Polymers, 137, 549–555. https://doi.org/10.1016/j.carbpol.2015.11.026

Zeng, L., Xiang, R., Fu, C., Qu, Z., & Liu, C. (2022). The Regulatory effect of chlorogenic acid on gut-brain function and its mechanism: A systematic review. *Biomedicine & Pharmacotherapy, 149*, Article 112831. https://doi.org/10.1016/j.biopha.2022.112831

Zhang, Y., Li, Y., Ren, X., Zhang, X., Wu, Z., & Liu, L. (2023). The positive correlation of antioxidant activity and prebiotic effect about oat phenolic compounds. *Food Chemistry, 402*, Article 134231. https://doi.org/10.1016/j.foodchem.2022.134231

Zhao, Y., Bi, J., Yi, J., Wu, X., Ma, Y., & Li, R. (2021). Pectin and homogalacturonan with small molecular mass modulate microbial community and generate high SCFAs via *in vitro* gut fermentation. *Carbohydrate Polymers, 269*, Article 118326. https://doi.org/10.1016/j.carbpol.2021.118326

Zhou, Z., Wang, D., Xu, X., Dai, J., Lao, G., Zhang, S., et al. (2022). Myofibrillar protein-chlorogenic acid complexes ameliorate glucose metabolism via modulating gut microbiota in a type 2 diabetic rat model. *Food Chemistry, 409*, Article 135195. https://doi.org/10.1016/j.foodchem.2022.135195

Zhu, B., Chen, Y., Chang, S., Qiu, H., & You, L. (2023). Degradation kinetic models and mechanism of isomaltooligosaccharides by hydroxyl radicals in UV/H_2O_2 system. *Carbohydrate Polymers, 300*, Article 120240. https://doi.org/10.1016/j.carbpol.2022.120240

Zhu, Q., & Wu, S. (2019). Water-soluble β-1,3-glucan prepared by degradation of curdlan with hydrogen peroxide. *Food Chemistry, 283*, 302–304. https://doi.org/10.1016/j.foodchem.2019.01.036